



## New look for an old molecule – Solid/solid phase transition in cholesterol monolayers

J.L. Fidalgo Rodriguez<sup>a</sup>, L. Caseli<sup>b</sup>, J. Minones Conde<sup>a</sup>, P. Dynarowicz-Latka<sup>c,\*</sup>

<sup>a</sup> Department of Physical Chemistry, Faculty of Pharmacy, University of Santiago de Compostela, Spain

<sup>b</sup> Institute of Environmental, Chemical and Pharmaceutical Sciences, Federal University of São Paulo, Brazil

<sup>c</sup> Faculty of Chemistry, Jagiellonian University, Kraków, Poland

### ARTICLE INFO

#### Keywords:

Cholesterol  
Langmuir monolayers  
Phase transition  
Molecular orientation  
Film thickness measurements  
PM-IRRAS

### ABSTRACT

Surface pressure ( $\pi$ ) – molecular area ( $A$ ) isotherms of cholesterol were precisely measured to get insight into the orientation of molecules in Langmuir monolayers, which allowed to obtain detailed information on their phase behaviour. This was possible from the detailed analysis of the interfacial compressibility modulus *versus* surface pressure ( $C_s^{-1} - \pi$ ) plots (obtained from the experimental surface pressure,  $\pi$  - area,  $A$  isotherms) and films thickness measurements (applying Brewster angle microscope, BAM) complemented with polarization-modulation infrared reflection-absorption spectroscopy (PM-IRRAS). At first glance, the isotherm for cholesterol is characterized by the major slope change of surface pressure *versus* area per molecule. However, a more detailed analysis showed the presence of a discontinuity and slope change both upon the compression and expansion of the monolayer. This discontinuity is more accurately reflected in the  $C_s^{-1} - \pi$  plot as a pseudo-plateau visible at  $\pi$  values between approximately 5 and 10 mN/m. This plateau was found to be temperature-dependent. Also, film thickness *versus* area plot ( $th-A$ ) exhibits a pseudo-plateau in this region of surface pressures, in which the monolayer thickness increased gradually from 1.15 nm to 1.5 nm. Interestingly, although cholesterol has been intensively investigated in Langmuir monolayers, the existence of such a plateau have been overlooked previously. By linking experimental thickness values with theoretical molecular conformations, we have identified the presence of this plateau to the solid-solid ( $S-S'$ ) second-order transition. Using 2D analog of Clausius-Clapeyron equation, the thermodynamic functions ( $\Delta H$  and  $\Delta S$ ) for this transition have been calculated. Based on monolayer experiments, the orientation of molecules in both solid phases was assumed to differ in the orientation of short alkyl chain attached to C17, which has additionally been confirmed with PM-IRRAS analysis.

### 1. Introduction

The arrangement of molecules in biological membranes is supposed to be strongly related to their biological function. Therefore, it is of utmost importance to have a detailed knowledge of possible changes of biomolecules tilt orientation, which may influence the strength of intermolecular interactions and - in consequence - modify membrane properties.

There are many reports in literature pointing to the important role of molecules' orientation in their behavior in biological membranes. Good examples are sterols. These molecules are vitally important constituents of biological membranes and therefore any change in their orientation may affect mechanical and biophysical properties of natural bilayers. It has been proved (Aittoniemi *et al.*, 2006) that any slight modification either in the tetracyclic ring system or in the short alkyl

chain attached to C17 in the sterol molecule influence on its tilt, which correlates with the sterol's ability to induce order in the biomembrane, which is of particular importance in rafts formation. It has been shown that cholesterol analogues, which are more tilted, are less effective in increasing membrane order and condensation. Other authors show that differences in chemical structure of sterols in the sterane ring are less important than the side chain structure. It has been shown that any modification in the side chain affects the geometry of a molecule as evidenced for  $\beta$ -sitosterol, stigmasterol and campesterol *versus* cholesterol (Berezin *et al.*, 2001). Namely, the presence of an additional methyl group (campesterol) or double bond ( $\beta$ -sitosterol, stigmasterol) as compared to cholesterol was found to increase the diameter of the molecule and shorten its length (Berezin *et al.*, 2001). These differences influenced interactions with other membrane lipids – as indicated in (Halling and Slotte, 2004) -  $\beta$ -sitosterol, stigmasterol and campesterol

\* Corresponding author.

E-mail address: [ucdynaro@cyf-kr.edu.pl](mailto:ucdynaro@cyf-kr.edu.pl) (P. Dynarowicz-Latka).

<https://doi.org/10.1016/j.chemphyslip.2019.104819>

Received 4 July 2019; Received in revised form 25 August 2019; Accepted 12 September 2019

Available online 13 September 2019

0009-3084/ © 2019 Elsevier B.V. All rights reserved.

interacted with phospholipids less favorably than cholesterol. Sitosterol and stigmasterol were also found to be less effective as compared to cholesterol in ordering the hydrocarbon chains of phospholipids (Hodzic et al., 2008).

All this proves that molecular orientation of molecules is of great importance in their biological activity. A method to get insight into molecular properties of membrane components is to measure macroscopic quantities to acquire information on microscopic scale, using a suitable membrane model. In this paper we have applied the Langmuir monolayer approach (Gaines, 1966) as artificial membrane model and carefully measured the macroscopic parameters (such as surface pressure and film thickness) of cholesterol monolayer and derived information on molecular orientation at particular stages of its compression. The obtained information was complemented with *in-situ* spectroscopic (PM-IRRAS) measurements.

Cholesterol (cholest-5-en-3 $\beta$ -ol) is known to be of a special biomedical significance. It is well known for its importance in regulating membrane biophysical properties. It regulates fluidity, permeability and surface density of biomembranes (Barenholz, 2002; Haines, 2001; Maxfield and Tabas, 2005). Moreover, it increases the order of phospholipids acyl chains and is vital in formation of lipid domains, called lipid rafts (Tabas, 2002; Krause and Regen, 2014). It is a precursor of steroid hormones, bile acids and vitamin D3 (Tabas, 2002; Miller, 1998; Salen and Shefer, 1983). Also, it protects the body from oxidative stress by forming oxysterols (Kulig et al., 2016). But cholesterol is not always beneficial to the body but - on the contrary - can be harmful to it. Most known unfavorable effect of cholesterol excess in blood are cardiovascular disorders.

Cholesterol is present in cell membranes of all mammals although different organelles contain different proportion of cholesterol (Lange and Ramos, 1983). Taking into account membrane asymmetry, in contrast to phospholipids, which distribution between inner and outer layers has well been established (Rothman and Lenard, 1977), the partition of cholesterol is still controversial. Red blood cell (RBC) membrane, which has been thoroughly investigated, may serve as an example. Early works indicate a higher content of cholesterol in the outer layer of the membrane (Fisher, 1976) while others suggest its predominance in the inner leaflet (Schroeder et al., 1991). Recent investigations postulate its homogeneous distribution between the two membrane layers (Müller and Herrmann, 2002). The difficulty in determining the distribution of cholesterol is due to the short time of transmembrane diffusion (flip-flop) (the half time of cholesterol molecule movement across the membrane layers at 37 °C is below 1 s (Steck et al., 2002)).

Cholesterol has long been investigated in Langmuir monolayers. Its amphiphilic structure and adequate hydrophilic-hydrophobic balance allow for stable Langmuir monolayer formation. As reviewed in a recent paper (Mangiarotti et al., 2019), monolayer from cholesterol forms very sharp surface pressure ( $\pi$ )-area (A) compression isotherm, indicative of a very compact, closely-packed high-density monolayer with high compressibility modulus ( $C_s^{-1}$ , defined below: Eq. (1)) characteristic of solid-like film, which is additionally proved with other characteristic parameters of cholesterol monolayer, such as high reflectivity at the Brewster angle and high values (above 300 mV at the maximum) of electric surface potential ( $\Delta V$ ). Interestingly, as rheological properties are concerned, the viscosity of cholesterol monolayers is comparable to liquid-expanded (LE) phases (Mangiarotti et al., 2019; Diaz et al., 2016). These exceptional, dualistic properties of cholesterol monolayers are of utmost importance, especially in incorporation of membrane-active molecules into biological membranes (Diaz et al., 2016).

Although the course of Langmuir monolayer from cholesterol has been well known for a long time, however, upon analysing thoroughly surface pressure ( $\pi$ ), compressibility modulus ( $C_s^{-1}$ ) and thickness (th) isotherms, we have identified discontinuities in these dependencies, related to changes in molecular conformations in the solid state, which have not been reported before, and confirmed them with PM-IRRAS.

Moreover, temperature dependence of the observed transition allowed for thermodynamic functions ( $\Delta H$  and  $\Delta S$ ) calculation using the modified Clausius-Clapeyron equation for second order transitions in two-dimensional systems.

## 2. Experimental

### 2.1. Materials

Cholesterol was purchased from Sigma (purity  $\geq$  99%) and was stored according to the supplier information. Chloroform and ethanol pre-analysis, used as spreading solvents, were supplied by Merck and used without further purification. The spreading of the solvents did not alter the surface tension of the water surface, indicating the absence of surface active impurities. Ultrapure water, used as subphase, was obtained from the Milli-Q Plus system (Millipore) (18.2 M $\Omega$  cm, pH 6). Spreading solution of cholesterol, prepared by dissolving the compound (0.15 – 0.20 mg/mL) in chloroform, were dropped onto the water subphase with a Microman-Gilson microsyringe precise to  $\pm$  0.2  $\mu$ l. 10 min were allowed for solvent evaporation before the compression has been initiated. The number of molecules spread on the subphase ( $4\cdot 10^{16}$  molecules) was kept constant in all the experiments.

### 2.2. $\pi$ -A isotherm measurements

Surface pressure ( $\pi$ ) - molecular area (A) isotherms were registered in a computer-controlled NIMA 601 standard-trough (Coventry, UK), placed on an antivibrational table, with a working surface area of 500 cm<sup>2</sup>, volume 300 mL, equipped with a Teflon barrier and a Whatman Chr 1 chromatography paper plate as the surface pressure sensor. Surface pressure was measured with an accuracy of  $\pm$  0.1 mN m<sup>-1</sup>. The subphase temperature (20, 25, 30, 35°C) was maintained with the accuracy of  $\pm$  0.1 °C by a circulating water system from Haake thermostat. In standard experiments, monolayers were compressed with a barrier speed of 50 cm<sup>2</sup> min<sup>-1</sup> (12.5 Å<sup>2</sup>·molecule<sup>-1</sup>·min<sup>-1</sup>) otherwise specified. Each experiment was repeated at least three times, and the reproducibility of the isotherms was  $\pm$  0.2 Å<sup>2</sup>·molecule<sup>-1</sup>.

### 2.3. Film thickness measurements

Measurements of film thickness were carried out on a floating monolayer using a Brewster Angle Microscope, BAM 2 Plus (NFT, Göttingen, Germany), mounted directly on the Nima trough and placed into a safety cabinet to protect against dust and air convection. The microscope was equipped with a 30 mW laser emitting *p*-polarized light with a wavelength of 532 nm, which was reflected off the air/water interface at the incident Brewster angle (53.1°). Under such conditions, the reflectivity of the *p*-polarized reflected beam ( $R_p$ ) is zero on pure water surface. However, when a monolayer is spread on the water surface, the refractive index of the medium changes, modifying the value of the Brewster angle and increasing the reflectivity of the reflected beam. This reflected beam passes through a focal lens into an analyzer at a known angle of incident polarization and finally to a CCD camera, which measures gray levels (GL) instead of the relative intensity (I). At the Brewster angle,  $I = R_p^2 = C \times (\text{th})^2$ , where I is the relationship between the reflected ( $I_r$ ) and incident ( $I_0$ ) light intensities ( $I = I_r/I_0$ ) and C is a constant. To measure film thickness (th), camera calibration is necessary to determine the relationship between GL and I. BAM 2 Plus automatically performs this calibration. In the calculation of cholesterol monolayer thickness from reflectivity data, the refraction index of the film was assumed to be 1.47, according to other authors (Lafont et al., 1998; Cadena-Nava et al., 2006; Pusterla et al., 2017).

### 2.4. Molecular configuration

The interpretation of the recorded thickness data was carried out by

associating these values with molecular configurations of cholesterol and stearic acid registered in the database of the US National Center for Biotechnology (NCBI) (2019) (<https://www.ncbi.nlm.nih.gov/>).

## 2.5. PM-IRRAS

For PM-IRRAS spectroscopy, the floating monolayers were spread at the water subphase adjusted to 20 °C and compressed up to the desired surface pressure by moving the barriers, and stopping them before the obtainment of the spectra. The stabilization of the surface pressure was monitored during the acquisition of the spectra and no additional movement of the barriers was needed to keep the surface pressure constant in order to avoid fluctuations of the compressional properties of the monolayer, as evidenced by high stability of cholesterol monolayer at different surface pressures at which the spectra were taken (Fig. S1, Supplemental files). The PM-IRRAS spectra were obtained using a KSV PMI 550 instrument (KSV Instruments, Ltd., Helsinki, Finland) at a fixed incidence angle of 76° and a minimum of 18,000 scans for each shown spectrum. Spectra with resolution of 4 cm<sup>-1</sup> were apodized with a triangular function and Fourier transformed with one level of zero filling.

## 3. Results and discussion

### 3.1. Langmuir monolayer experiments

#### 3.1.1. Surface pressure ( $\pi$ )-area ( $A$ ) isotherms and compressibility modulus ( $C_s^{-1}$ ) - surface pressure ( $\pi$ ) plots

Fig. 1 shows the  $\pi$ - $A$  isotherm for cholesterol monolayer obtained by spreading  $4 \times 10^{16}$  molecules on deionized water, pH 6, at different subphase temperatures (20; 25, 30 and 35 °C), applying standard compression speed of 12.5 Å<sup>2</sup> molecule<sup>-1</sup> min<sup>-1</sup> (50 cm<sup>2</sup> min<sup>-1</sup>). It is well known that cholesterol has a highly condensed monolayer at the air/water interface, with a limiting area of 39 Å<sup>2</sup> per molecule, which is in a good agreement with values reported elsewhere. For example, some authors (Motomura et al., 1976; Takano et al., 1997) obtained a value of 38.5 Å<sup>2</sup> molecule<sup>-1</sup>, while the values of 38.1 Å<sup>2</sup> molecule<sup>-1</sup> (Kodama et al., 2004) and  $\sim 39$  Å<sup>2</sup> molecule<sup>-1</sup> (Baglioni et al., 1985; Ali et al., 2010) were recorded by other researchers. The other characteristic monolayer parameter is the collapse surface pressure, which value is a measure of the force at which the film adheres to the aqueous substrate. Cholesterol film collapses at an area per molecule of 37 Å<sup>2</sup> and at the surface pressure of  $44 \pm 1$  mN m<sup>-1</sup>; both values are consistent with those reported elsewhere (Baglioni et al., 1985; Seoane et al., 2000;

Dynarowicz-Latka and Hąc-Wydro, 2004; Korchowiec et al., 2006; Giri et al., 2017; Mangiarotti et al., 2019).

Looking at the overall  $\pi$ / $A$  isotherm it seems that the monolayer molecules are transformed directly from gas-solid coexistence (at  $\pi \approx 0$  mN/m) to the solid (S) state, where no visible discontinuity was observed. However, a detailed analysis reveals the change of inclination within the solid state as seen in the inset of Fig. 1. Since cholesterol isotherm has usually been presented in literature in a large scale of areas/molecule, this kink has been overlooked previously.

First of all, it must be proved that any subtle discontinuities visible in the course of the  $\pi$ / $A$  isotherm are not caused by the presence of impurities. Therefore, in addition to using a high purity cholesterol sample, and applying a rigorous cleaning procedures during monolayer experiments, each isotherm was repeated at least 3 times to ensure reproducible results to  $\pm 0.2$  Å<sup>2</sup>. The change of slope was found to be persistent in a series of isotherms and appeared both upon film compression and expansion (Fig. S2, Supplemental files). All these experiments prove that the observed discontinuity is not an artifact. Different compression rates applied to compress the monolayer were found not to alter the region of transition (Fig. S3 A, Supplemental files).

To get insight into this change of the isotherms inclination within the monolayer solid state, values of the compressibility moduli have been calculated from the isotherm data points. It is well known that the physical state of monolayers can be analysed more precisely with the compressibility modulus ( $C_s^{-1}$ ), which is reciprocal of the two-dimensional compressibility, also called “surface elasticity” (Miller and Liggie, 2009), defined as:

$$C_s^{-1} = -A \left( \frac{d\pi}{dA} \right) \quad (1)$$

wherein  $A$  denotes the area per molecule at a given surface pressure ( $\pi$ ). Compressibility modulus reflects the variations in the physical state of monolayers and molecular arrangements. For liquid expanded (LE) films,  $C_s^{-1}$  lies between 12.5 and 50 mN/m; for the liquid-condensed (LC) from 50 to 250 mN/m, and above 250 mN/m solid state is observed (Davies and Rideal, 1963; Anwender et al., 1988).

$C_s^{-1}$ - $\pi$  plots for cholesterol monolayers at different temperatures are shown in Fig. 2A. A plateau is observed at  $\pi$  values between approximately 5 mN/m and 10 mN m<sup>-1</sup>, where the compressibility moduli values changes approximately from 365 to 465 mN/m, depending on subphase temperature (a linear relationship was obtained as shown in Fig. S4, Supplemental files). In some other papers showing the plots of  $C_s^{-1}$  vs  $\pi$ , based on experiments from different labs, this plateau

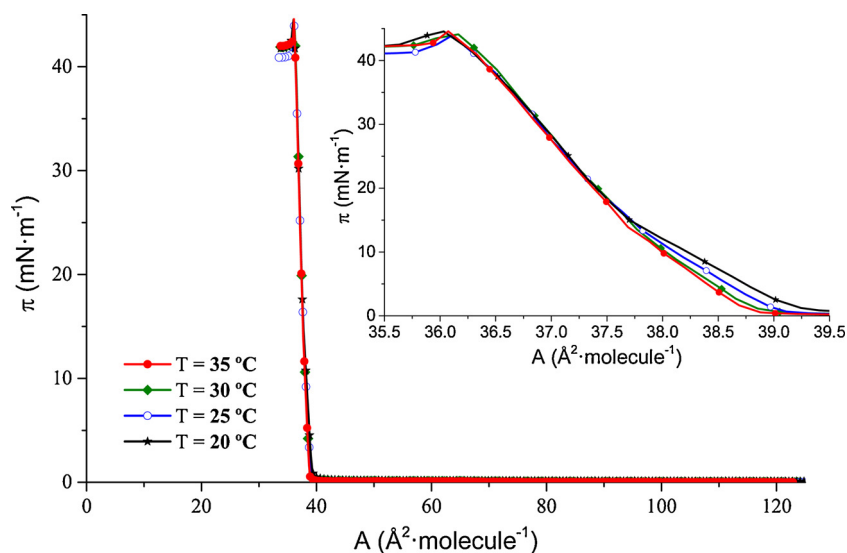


Fig. 1.  $\pi$ - $A$  isotherms for cholesterol monolayers obtained at different subphase temperatures. Inset: The change of inclination in the  $\pi$ / $A$  isotherm.

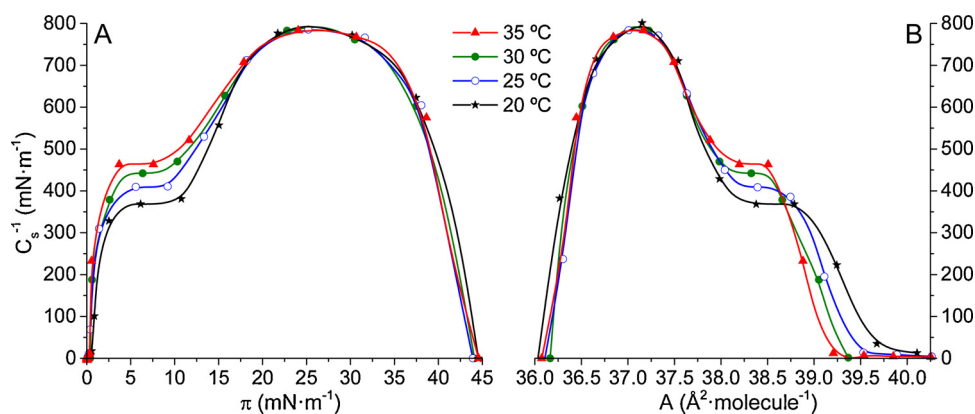


Fig. 2. (A) Compressibility modulus ( $C_s^{-1}$ )-surface pressure ( $\pi$ ), and (B) compressibility modulus-area per molecule ( $A$ ) dependences for cholesterol monolayers at different subphase temperatures.

is visible (see for example Sabatini et al., 2008; Makyla and Paluch, 2009; Telesford et al., 2015; Mangiarotti et al., 2019), however, none of the authors commented on this. As proved in Fig. S3 B, Supplemental files, the use of different compression speeds, especially within the range of 10-50  $\text{cm}^2/\text{min}$ , does not influence the plateau in any significant way. This plateau can be attributed to a solid - solid (S-S') phase transition, as shown later on. After the plateau, the compressibility modulus increases as the compression continues until maximum value is obtained ( $C_s^{-1} \sim 799 \text{ mN}\cdot\text{m}^{-1}$ , at  $\pi = 27 \text{ mN}\cdot\text{m}^{-1}$ ). This maximum value corresponds to film molecules in their solid state (Davies and Rideal, 1963; Anwender et al., 1988). Similar results of the maximum compressibility moduli values for cholesterol monolayer can be found in literature (Dynarowicz-Latka and Hąc-Wydro, 2004; Hąc-Wydro and Wydro, 2007), although smaller values have also been reported (Makyla and Paluch, 2009; Mangiarotti et al., 2019). These discrepancies can be due to different experimental conditions applied (different spreading solvent, high compression speed, etc). At the surface pressure of 43-44  $\text{mN}\cdot\text{m}^{-1}$  (depending on temperature), the compressibility modulus curve goes to zero, which corresponds to the monolayer collapse, seen in the  $\pi/A$  isotherm as a characteristic "spike".

The presence of a phase transition in Langmuir monolayers can be detected – in the majority of cases - classically, upon a detailed analysis of the course of the  $\pi/A$  isotherms, which reveals the presence of discontinuities, such as plateau region(s) or kink(s). These singularities in the isotherm enable to distinguish the order of the phase transition (Kaganer et al., 1999). The presence of plateau regions in the  $\pi/A$  isotherms (which are not always perfectly horizontal) - that reflect in the  $C_s^{-1}$  vs  $\pi$  plots as minima – suggest first order phase transition (like for example LE-LC transition for long-chain carboxylic acids (Pallas and Pethica, 1985) whereas the kinks on the isotherms imply second order transitions, like in the present case of cholesterol monolayer. In some cases, phase transition cannot be detected in the isotherm as exemplified by a transition between two condensed phases of some fatty acid monolayers (Overbeck and Möbius, 1993). In the case of cholesterol, the detected transition S-S' can therefore be considered as the second order.

Thermodynamic functions for the first order phase transition (having a plateau on the  $\pi/A$  isotherm) can be calculated using 2D analog of the Clausius-Clapeyron equation (Motomura, 1980; Miñones et al., 1993; Wnętrzak et al., 2019 and references therein):

$$\Delta H = [(d\pi_t/dT) - (d\gamma/dT)]T\Delta A_t \quad (2)$$

where  $\Delta H$  and  $\Delta A$  are changes in molar heat and molecular area, respectively, for a transition at constant temperature  $T$  and constant surface pressure  $\pi_t$ ;  $(d\pi_t/dT)$  is the slope of the dependence  $\pi_t(T)$ , obtained from  $\pi(A)$  isotherms recorded at different temperatures, and  $\gamma$  is

the surface tension of water. The value of  $d\gamma/dT$  (for temperatures between 5 and 40 °C) equals  $-0.153 \text{ mN}\cdot\text{m}^{-1} \text{ K}^{-1}$  (Miñones et al., 1993) and  $\Delta A_t = A_e - A_i$ , where  $A_e$  is the area per molecule at the end of plateau and  $A_i$  - at its beginning.

For the second order transition, like in the case of cholesterol, the plateau appears in the dependence of  $C_s^{-1} = f(\pi)$ , and the thermodynamic functions for such a transition can be estimated using the modified Clausius-Clapeyron equation.

Since  $(d\pi/dT) = (d\pi/dA)(dA/dT)$  and from the definition of compressional moduli (Eq. (1)):  $(d\pi/dA) = -(C_s^{-1}/A)$ , we obtain  $d\pi/dT = -(C_s^{-1}/A)(dA/dT)$ .

Thus, the Clausius-Clapeyron equation can be expressed in the following form:

$$\Delta H = [- (C_s^{-1}/A)(dA/dT) - (d\gamma/dT)]T\Delta A_t \quad (3)$$

From Fig. 3 it is seen that  $(dA/dT)$  value (i.e. the slope of individual  $A(T)$  straight line) at a selected surface pressure within the transition (5; 7.5; 10  $\text{mN}\cdot\text{m}^{-1}$ ) is roughly the same. In particular, for the value of surface pressure corresponding to the mid plateau (7.5  $\text{mN}\cdot\text{m}^{-1}$ ) it equals  $-0.01863 (\text{Å}^2\cdot\text{molecule}^{-1}\cdot\text{deg}^{-1})$ .

Introducing into the above Eq. (3) the following values obtained at 25 °C:  $C_s^{-1} = 409.33 \text{ mN}\cdot\text{m}^{-1}$ ,  $A = 38.35 \text{ Å}^2\cdot\text{molecule}^{-1}$  (corresponding to the mid plateau) and  $\Delta A_t = -0.55 \text{ Å}^2\cdot\text{molecule}^{-1}$ , the value of  $\Delta H$  equals  $-347 \text{ J}\cdot\text{mol}^{-1}$  and thus the entropy change ( $\Delta S = \Delta H/T$ ) for the S-S' phase transition of cholesterol film reads

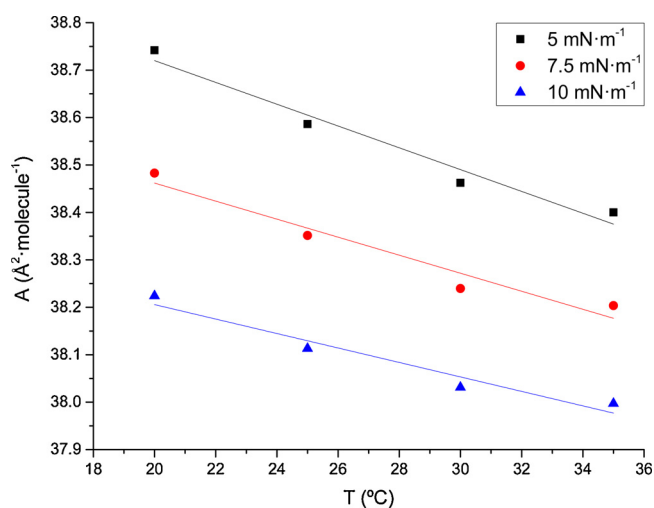


Fig. 3. The dependence of molecular area ( $A$ ) of cholesterol as a function of temperature ( $T$ ) for selected surface pressures (5; 7.5; 10  $\text{mN}\cdot\text{m}^{-1}$ ) within the transition region. The values were taken from  $\pi/A$  isotherm (inset of Fig. 1).

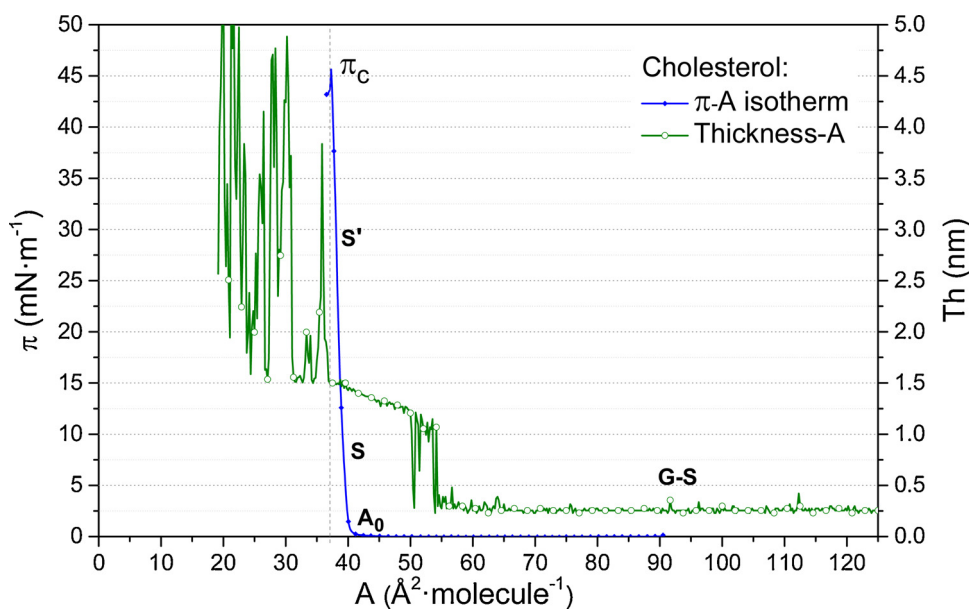


Fig. 4. Surface pressure- area (blue) and thickness-area (green) isotherms of cholesterol monolayer at 20 °C.

-1.16 J·mol<sup>-1</sup> K<sup>-1</sup>). The calculated values of  $\Delta H$  are negative at all the temperatures studied, which means that the process occurring along the plateau is exothermic. The entropy change is small, but negative, which means that cholesterol in the state S' is more ordered than in the S state, which is logical.

### 3.1.2. Monolayer thickness and molecular configuration

Values of the monolayer thickness (th) upon film compression allowed to obtain information about changes in molecular orientation of cholesterol at the air/water interface upon compression. Fig. 4 shows the monolayer thickness (th) versus the area per molecule (A) plot together with the corresponding  $\pi$ -A isotherm for comparison.

As it can be seen, the relative intensity signal that enabled film thickness measurements is triggered off at larger area (so-called *critical area*) compared to surface pressure lift-off, similarly to other parameters, such as electric surface potential, lateral conductivity or UV-VIS absorbance (reviewed in Oliveira et al., 2004). However, critical area for the above-mentioned parameters does not coincide with each other. This is simply because other phenomena are responsible for surface pressure rise as compared to other parameters. While surface pressure is sensitive to the density of film molecules, relative intensity signal depends on film molecules tilt angle (Ducharme et al., 1985), whereas surface potential or lateral conductivity start to change when the hydrogen bonds between film molecules and water begin to break (Morgan et al., 1991).

In the thickness-area curve, four regions are observed: a) at large areas, when the monolayer exhibits the G-S phase transition, the average value of the film thickness remains constant (of approximately 0.25 nm) with monolayer compression; b) first abrupt increase of film thickness, from 0.25 nm to 1.15 nm, is related to the surface pressure rise; c) upon compression, a plateau region begins, in which the film thickness continues to increase gradually until reaching a value of 1.5 nm; d) at the end of this plateau, which coincides with the monolayer collapse, there is again a sudden increase of film thickness, which gets stabilized at the average value of approximately 3 nm in a region where large noise peaks of thickness are observed, ranging from 1.5 nm to 4.5 nm.

The first sharp increase of monolayer thickness from 0.25 nm to 1.15 nm can be attributed to the beginning of the solid surface phase, which is also visualized in the  $\pi$ -A isotherm as a further increase of the surface pressure from  $\pi = 0$  to ca. 43 mN m<sup>-1</sup> (molecular area  $\sim$

39 Å<sup>2</sup>). On the other hand, a plateau spanning between 1.15 nm and 1.5 nm in the thickness curve, preceding the monolayer collapse, also coincides with the plateau observed in the C<sub>s</sub><sup>-1</sup>- $\pi$  curve (Fig. 2A) at  $\pi$  values between 5 and 10 mN·m<sup>-1</sup> and can be attributed to a conformational change of cholesterol molecule, as shown below.

In order to determine the conformation of cholesterol molecule in different surface phases of its monolayer spread at the air/water interface, we take - as a reference - the carbon atom C3 of the cyclopentanoperhydrophenanthrene (sterane) group, which is bound to the OH group anchored in the water subphase, and we calculate the theoretical distance (*d*) between this C3 atom and the C17 atom attached to the flexible aliphatic side chain with 8 carbon atoms. For this theoretical *d* calculation, data from the US National Center for Biotechnology Information (NCBI), corresponding to the cholesterol molecular conformation, were used. The obtained theoretical *d* value was 0.87 nm. On the other hand, depending on whether the flexible isoocetyl chain is horizontally or vertically oriented in respect to the water surface, the total theoretical length of cholesterol molecule was estimated to be either 1.12 nm (horizontal orientation) or 1.42 nm (vertical orientation), respectively. These values practically coincide with the experimental thickness data obtained from th- $\pi$  curve. Indeed, the experimental film thickness value at the beginning of the plateau (1.15 nm), is similar to the length of cholesterol molecule with side hydrocarbon chain oriented horizontally in relation to the water surface and the sterane ring vertically oriented to the water surface (1.12 nm). On the other hand, the experimental value of 1.5 nm, corresponding to the monolayer thickness at the end of the plateau almost coincides with the maximum possible theoretical length of cholesterol molecule with its side acyl chain vertically oriented in respect to the water surface (1.42 nm).

It is also possible that cholesterol molecule adopts other configurations, i.e. the sterane ring is not oriented exactly vertically to the water surface, or the aliphatic moiety is not completely horizontally oriented, but is inclined at a certain angle to the horizontal axis. However, these options were rejected assuming that they are less stable from the thermodynamic point of view.

Finally, along the gas-solid phase transition, the monolayer thickness values remain constant with compression (th<sub>G-S</sub> = 0.25 nm) until the surface pressure lift-off. To achieve such a low thickness value, cholesterol molecule must be tilted with respect to the water subphase (Oakes and Domene, 2018).

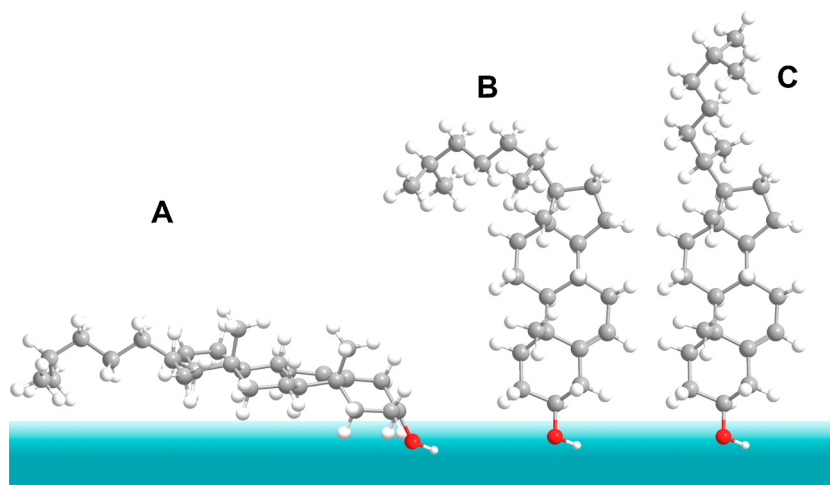


Fig. 5. Change of cholesterol molecule orientation upon compression – explanation in the text.

With these data, the molecular conformations for cholesterol along film compression are illustrated in Fig. 5. During the gas-solid transition, as already indicated above, it is postulated that the film molecules are tilted in respect to the water surface, with their aliphatic end-to-end moiety parallel to the aqueous substrate (Fig. 5A). This particular orientation explains a low thickness value obtained in this region (0.25 nm). At the end of this phase transition (gas – solid), it is assumed that there is a change of orientation of the sterane ring (with the aliphatic chain remaining in horizontal position) from the initial tilted position to the vertical one at the beginning of the plateau (Fig. 5B). This reorientation of the sterane corresponds to a sudden and simultaneous increase in the thickness and surface pressure observed in Fig. 4. Then, as the compression proceeds along the pseudo-plateau, the aliphatic side chain of cholesterol is gradually reoriented to vertical position until the onset of collapse, at which both the sterane ring and the terminal alkyl moiety are vertically oriented to the air/water interface (Fig. 5C).

The results of our experiments confirm that the collapse of cholesterol monolayer follows the mechanism proposed by Ries (Ries, 1979), according to which at the collapse a folding and subsequent bending of the monolayer occurs and a trilayer (i.e. bilayer on the top of original monolayer) is formed. Namely, the over-pressure exerted on cholesterol monolayer causes the film folding out of the aqueous subphase, provoking the surface pressure to fall sharply from ca.  $44 \pm 1 \text{ mN m}^{-1}$  (Fig. 1). Simultaneously, due to the folding of the monolayer towards the air, a sharp increase of the thickness occurs, as shown in Fig. 4. If the film is rigid, as it occurs in the case of cholesterol, the formed bilayer, which vertically protrudes out of water, becomes tilted and breaks, resulting in formation of a bilayer on the top of a monolayer. These three-dimensional trilayer structures are formed continuously throughout the collapse while the surface pressure remains constant. However, the recorded thickness shows oscillations (noise peaks) between the value corresponding to that of the monolayer (thickness of 1.5 nm) and that of the trilayer structure (4.5 nm) (Fig. 4) although the average thickness value remains constant in this region.

### 3.1.3. BAM images and morphology

Brewster angle microscope enables morphological analysis of monolayers at different stages of their compression. Texture of cholesterol monolayers have already been published, and the images obtained by us (Fig. S5, Supplemental files) are in agreement with literature; i.e. at the gas-solid phase transition (at 20 °C), a fluid-like foam texture was observed, similar to those shown by other authors (de Wolf et al., 1999; Viswanath and Suresh, 2004; Cadena-Nava et al., 2006), formed by large, gray domains of cholesterol, surrounded by water subphase (black background), which - in some cases - is embedded

inside the domains. Upon compression within this region, these domains merge (expelling the water from their inside), increase in size and cover most of the microscope field of view (images not shown). During the abrupt increase in surface pressure, when the monolayer reaches the solid state, the image looks completely homogeneous (Figure S5 B, taken at  $\pi = 5 - 40 \text{ mN m}^{-1}$ ). This homogeneity is due to the fact that in this state the film is isotropic as a consequence of the orientation change of the molecules from the tilted to the vertical position, as mentioned before, so that the reflected light is *p*-polarized, and the incident light as well, resulting in uniform field of observation. The appearance of this image is maintained along the solid phase and increase of subphase temperature (to 25, 30 or 35 °C) does not cause any visible changes. Film's homogeneity disappears at the onset of film collapse, where the existence of small white dots (Figure S5 C, taken at  $44 \text{ mN m}^{-1}$ ) is observed, corresponding to the initial folding of the monolayer outside the interface. In the post-collapse one can observe three-dimensional elongated, small "rod" crystalline structures (Figure S5 D), with a variable size (ranging from 4 to 7  $\mu\text{m}$ ), corresponding to the trilayer structures existing in this region. These very bright three-dimensional "rods" are responsible for the existence of large noise peaks of thickness seen in Fig. 4. Indeed, when the polarized light of the microscope reach them, a very intense reflected signal is obtained, which is followed by a weak signal when BAM reflected light comes from the water covered by the monolayer. The greater intensity of the light reflected by the three-dimensional "rods" is due to their thickness, since the reflectivity (ratio of the reflected light intensity to that of the incident light) of the *p*-polarized reflected light is proportional to the square of the thickness.

### 3.1.4. PM-IRRAS spectroscopy

PM-IRRAS spectra were taken in four conditions, at 20 °C, as shown in Fig. 6: at 0 mN/m (gaseous state), 3 mN/m (S state), 17 mN/m (S' state), and collapse. Complementary data at 30 °C are shown in the Supplemental files (Fig. S5). The main bands encountered in this region are attributed to C–H stretches. Bands centered at approximately  $2855\text{--}2860 \text{ cm}^{-1}$  and  $2915\text{--}2920 \text{ cm}^{-1}$  are attributed, respectively, to symmetric and antisymmetric stretches for  $\text{CH}_2$ , and those at 2888, 2944 and  $2974 \text{ cm}^{-1}$  are attributed to symmetric, in-skeletal plane antisymmetric and out-of-skeletal antisymmetric stretches for  $\text{CH}_3$ , respectively. In the collapsed monolayer, for both temperatures, the peaks for antisymmetric  $\text{CH}_2$  stretches are badly defined, and particularly in the region between 2880 and  $2850 \text{ cm}^{-1}$  the bands overlap each other, which causes low distinction between them, except for the band at  $2858 \text{ cm}^{-1}$  (attributed to symmetric stretches in  $\text{CH}_2$ ). The distinction between the spectrum of the collapse film and other states occurs probably because of the disorganized state reached by the monolayer.

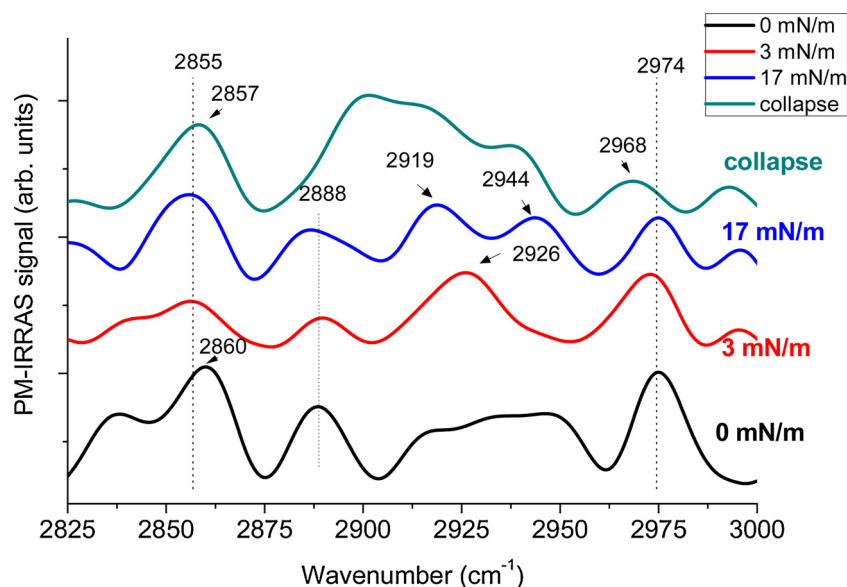


Fig. 6. PM-IRRAS spectra for cholesterol monolayer at 20 °C.

Overlapping of some bands also occurs at 0 mN/m, at which the monolayer is encountered in the gaseous state. For instance, the region for the asymmetric stretches in  $\text{CH}_2$  shows indistinguishable bands at low surface pressures. Furthermore, the band attributed to symmetric stretches in  $\text{CH}_3$  ( $2855\text{--}2860\text{ cm}^{-1}$ ) appears to be only slightly changed upon compression, being difficult to correlate to any significant structural change in the monolayer based on this region of the spectrum.

However, focusing on the antisymmetric stretching mode for  $\text{CH}_2$  at the surface pressure values of 3 and 17 mN/m, corresponding to S and S' states respectively, the band peak shifts from 2926 to 2919  $\text{cm}^{-1}$ . As the frequencies of these bands are highly sensitive to conformation and respond to changes in the *trans-gauche* ratio of carbon-carbon bonds in the acyl chains, the shift of the absorption maxima for these bands to lower frequencies is therefore related to the decrease of the proportion of gauche conformers (Mendelsohn et al., 2010), i.e., the conformational order of monolayer increases from 3 to 17 mN/m. These data therefore corroborate with the model proposed previously above since the alkyl chains should go with compression from position with more gauche defects (tilted) to that with more *trans* conformations (vertical). For the other monolayer states examined (0 mN/m and collapse), this band is less distinct, being broadened or overlapped by other bands, which is in agreement with the lower order expected by the cholesterol monolayer in this state. Additionally, particularly for the collapse state, the band centered in  $2888\text{ cm}^{-1}$  is also indistinct.

It is important to mention that in the  $1000\text{--}1800\text{ cm}^{-1}$  region, where some bands related to hydrophilic groups may appear (such as C=C and C-O vibrations), no significant change in the profile of the bands were observed upon compression (not shown), which leads to the conclusion that the differences in the S and S' phases should be related to the change in orientation of the alkyl chain attached to C17, from more inclined to the interface to more vertical, while the steroid ring is not influenced (Fig. 5 B versus C). At 30 °C (Supplemental files, Fig. S6), although some minor changes in the profile of the spectra occur, in general the main result is similar: the antisymmetric band for  $\text{CH}_2$  was shifted to lower wavenumbers when the monolayer goes from 3 to 17 mN/m as a consequence of the increase of *trans* conformers.

#### 4. Conclusions

Despite over 2 centuries of intensive research involving cholesterol, this key biomolecule still remains a subject of scientific interest and investigations. In this paper we have reported on a solid-solid phase

transition in Langmuir monolayers from cholesterol, which – surprisingly – has been overlooked in former studies involving this molecule, contrary to long-chain alcohols (Lawrie and Barnes, 1994; and references therein), fatty acids or esters, as reviewed by (Kaganer et al., 1999), or biomolecules, like for example ceramides (Fanani and Maggio, 2010; Fanani et al., 2018) for which discontinuities in Langmuir isotherms have been detected, suggesting rich polymorphism of their condensed phases.

Detailed film thickness measurements together with spectroscopic analysis revealed that the difference in orientation of cholesterol molecules in both solid phases is related to a different tilt of flexible iso-octyl chain attached to C17. It has been well recognized that any change in biomolecule's tilt may modulate membrane mechanical and biophysical properties and influence the functioning of other molecules (e.g. proteins). The change of enthalpy for the S-S' transition in cholesterol monolayer is small in comparison to the first order phase transitions (LE-LC) observed in long-chain carboxylic acids (Pallas and Pethika, 1985) or phospholipids (such as DPPC and DPPG (Phillips and Chapman, 1968; Vollhardt et al., 2000) or POPE (Borrell and Domenech, 2017)) for which  $\Delta H$  was in order of a dozen or so kJ/mol. This small value evidences that the molecular conformations of cholesterol in S and S' condensed phases are very similar, contrary to what occurs in LE-LC or LC-S phase transitions. As compared to the second order S\*-S (analogous to L<sub>2</sub>-S, according to Harkins-Stenhagen nomenclature) transition in octadecanol monolayer, there is reasonable agreement, i.e.  $\Delta H$  and  $\Delta S$  were estimated to be also very small and negative (Lawrie and Barnes, 1994).

We do believe that the described transition in cholesterol monolayers will draw attention to researchers investigating further this molecule.

#### Acknowledgements

The authors are indebted to Prof. Jose Miñones Trillo (University of Santiago de Compostela, Spain) for helpful discussions.

#### Appendix A. Supplementary data

Supplementary material related to this article can be found, in the online version, at doi:<https://doi.org/10.1016/j.chemphyslip.2019.104819>.

## References

- Aittoniemi, J., Róg, T., Niemela, P., Pasenkiewicz-Gierula, M., Karttunen, M., Vattulainen, I., 2006. Tilt: major factor in sterols ordering capability in membranes. *J. Phys. Chem. B* 110, 25562–25564.
- Ali, M.H., Kirby, D.J., Mohammed, A.R., Perrie, Y., 2010. Solubilisation of drugs within liposomal bilayers: alternatives to cholesterol as a membrane stabilising agent. *J. Pharm. Pharmacol.* 62, 1646–1655.
- Anwander, A.E., Grant, R.P.J.S., Letcher, T.M., 1988. Interfacial phenomena. *Chem. Ed.* 65, 608–614.
- Baglioni, P., Cestelli, G., Dei, I., Gabrielli, G., 1985. Monolayers of cholesterol at water air interface – mechanism of collapse. *J. Colloid Interface Sci.* 104, 143–150.
- Barenholz, Y., 2002. Cholesterol and other membrane active sterols: from membrane evolution to “rafts”. *Prog. Lip. Res.* 41, 1–5.
- Berezin, M.Yu., Dzenitis, J.M., Hughes, B.M., Ho, S.V., 2001. Separation of sterols using zeolites. *Phys. Chem. Chem. Phys.* 3, 2184–2189.
- Borrell, J.H., Domenech, O., 2017. Critical temperature of 1-palmitoyl-2-oleoyl-*sn*-glycero-3-phosphoethanolamine monolayers and its possible biological relevance. *J. Phys. Chem. B* 121, 6882–6889.
- Cadena-Nava, R.D., Martín-Mirones, J.M., Vázquez-Martínez, E.A., Roca, J.A., Ruiz-García, J., 2006. Direct observations of phase changes in Langmuir films of cholesterol. *Rev. Mex. Física* 52, 32–40.
- Davies, J.T., Rideal, E.K., 1963. *Interfacial Phenomena*. Academic Press, New York.
- de Wolf, C., Leporati, S., Klingner, R., Brezesinski, G., 1999. Phase separation in phosphatidylinositol/phosphatidylcholine mixed monolayers. *Chem. Phys. Lipids* 97, 129–138.
- Diaz, Y.D.Z., Mottola, M., Vico, R.V., Wilke, N., Fanani, M.L., 2016. *Langmuir* 32, 587–595.
- Ducharme, D., Saless, C., Leblanc, R.M., 1985. Ellipsometric studies of rod outer segment phospholipids at the nitrogen-water interface. *Thin Solid Films* 132, 83–90.
- Dynarowicz-Latka, P., Hąc-Wydro, K., 2004. Interactions between phosphatidylcholines and cholesterol in monolayers at the air-water interface. *Colloids Surf. B* 37, 21–25.
- Fanani, M.L., Maggio, B., 2010. Phase state and surface topography of palmitoyl-ceramide monolayers. *Chem. Phys. Lipids* 163, 594–600.
- Fanani, M.L., Busto, J.V., Sot, J., Abad, J.L., Fabrias, G., Saiz, L., Vilar, J.M.G., Goni, F.M., Maggio, B., Alonso, A., 2018. Clearly detectable, kinetically restricted solid-solid phase transition in cis-ceramide monolayer. *Langmuir* 34, 11749–11758.
- Fisher, K.A., 1976. Analysis of membrane halves: cholesterol. *Proc. Natl. Acad. Sci. U. S. A.* 73, 173–177.
- Gaines, G.L., 1966. *Insoluble Monolayers at Liquid-Gas Interfaces*. Interscience, Ed, New York.
- Giri, R.P., Chakrabarti, A., Mukhopadhyay, M.K., 2017. Cholesterol-induced structural changes in saturated phospholipid model membranes revealed through X-ray scattering technique. *J. Phys. Chem. B* 121, 4081–4090.
- Hąc-Wydro, K., Wydro, P., 2007. The influence of fatty acids on model cholesterol/phospholipid membranes. *Chem. Phys. Lipids* 150, 66–81.
- Haines, T.H., 2001. Do sterols reduce proton and sodium leaks through lipid bilayers? *Prog. Lip. Res.* 40, 299–324.
- Halling, K.K., Slotte, J.P., 2004. Membrane properties of plant sterols in phospholipid bilayers as determined by differential scanning calorimetry, resonance energy transfer and detergent-induced solubilization. *BBA Biomembranes* 1664, 161–171.
- Hodzic, A., Rappolt, M., Amenitsch, H., Laggner, P., Pabst, G., 2008. Differential modulation of membrane structure and fluctuations by plant sterols and cholesterol. *Biophys. J.* 94, 3935–3944.
- Kaganer, V.M., Möhwald, H., Dutta, P., 1999. Structure and phase transitions in Langmuir monolayers. *Rev. Mod. Phys.* 71, 779–819.
- Kodama, M., Shibata, O., Nakamura, S., Lee, S., Sugihara, G., 2004. A monolayer study of three mixed systems of dipalmitoyl phosphatidyl choline with cholesterol, cholesterol and stigmaterol. *Colloids Surf. B Biointerfaces* 33, 211–216.
- Korchowiec, B., Paluch, M., Corvis, Y., Rogalska, E., 2006. A Langmuir film approach to elucidating interactions in lipid membranes: 1,2-dipalmitoyl-*sn*-glycero-3-phosphoethanolamine/cholesterol/metal cation systems. *Chem. Phys. Lipids* 144, 127–136.
- Krause, M.R., Regen, S.L., 2014. The structural role of cholesterol in cell membranes: from condensed bilayers to lipid rafts. *Acc. Chem. Res.* 47, 3512–3521.
- Kulig, W., Cwiklik, L., Jurkiewicz, P., Rog, T., Vattulainen, I., 2016. Cholesterol oxidation products and their biological importance. *Chem. Phys. Lipids* 199, 144–160.
- Lafont, S., Rapaport, H., Sömjen, G.J., Renault, A., Howes, P.B., Kjaer, K., Als-Nielsen, J., Leiserowitz, L., Lahav, M., 1998. Monitoring the nucleation of crystalline films of cholesterol on water and in the presence of phospholipid. *J. Phys. Chem. B* 102, 761–765.
- Lange, Y., Ramos, B.V., 1983. Analysis of the distribution of cholesterol in the intact cell. *J. Biol. Chem.* 258, 15130–15134.
- Lawrie, G.A., Barnes, G.T., 1994. Octadecanol monolayers: the phase diagram. *J. Colloid Interface Sci.* 162, 36–44.
- Makyla, K., Paluch, M., 2009. The linoleic acid influence on molecular interactions in the model of biological membrane. *Colloids Surf. B Biointerfaces* 71, 59–66.
- Mangiarotti, A., Galassi, V.V., Puentes, E.N., Oliveira, R.G., Del Popolo, M.G., Wilke, N., 2019. Hopanoids like sterols form compact but fluid films. *Langmuir* 35, 9848–9857.
- Maxfield, F.R., Tabas, I., 2005. Role of cholesterol and lipid organization in disease. *Nature* 438, 612–621.
- Mendelsohn, R., Mao, G., Flach, C.R., 2010. Infrared reflection-absorption spectroscopy: principles and application to lipid-protein interaction in Langmuir films. *Biochim. Biophys. Acta-Biomembranes* 1798, 788–800.
- Miller, W.L., 1998. Molecular biology of steroid hormone synthesis. *Endocr. Rev.* 9, 295–318.
- Miller, R., Liggie, L., 2009. Chapter 11: interfacial reology. *Compressibility of Langmuir Monolayers*. CRC Press p.475.
- Miñones, J., Yebra-Pimentel, E., Iribarnegaray, E., Conde, O., Casas, M., 1993. Influence of pH and temperature on poly(isobutylcyanoacrylate) monolayers. *Colloids Surf. A* 76, 101–108.
- Morgan, H., Taylor, D.M., Oliveira Jr, O.N., 1991. *Biochim. Biophys. Acta* 1062, 149–150.
- Motomura, K., 1980. Thermodynamics of interfacial monolayers. *Adv. Colloid Interface Sci.* 12, 1–42.
- Motomura, K., Terazono, T., Matuo, H., Matuura, R., 1976. Mixed monolayers of cholesterol with fatty acids. *J. Colloid Interface Sci.* 57, 52–57.
- Müller, P., Herrmann, A., 2002. Rapid transbilayer movement of spin-labeled sterols in human erythrocytes and in liposomes. *Biophys. J.* 82, 1418–1428.
- National Center for Biotechnology Information, 2019. U.S. National Library of Medicine. <https://www.ncbi.nlm.nih.gov/>.
- Oakes, V., Domene, C., 2018. Stereospecific interactions of cholesterol in a model cell membrane: implications for the membrane dipole potential. *J. Membr. Biol.* 251, 507–519.
- Oliveira, O.N.Jr., Riul, A.Jr., Leite, V.B.P., 2004. *Braz. J. Phys.* 34, 73–83.
- Overbeck, G.A., Möbius, D., 1993. A new phase in the generalized phase-diagram of monolayer films of long-chain fatty acids. *J. Phys. Chem.* 97, 7999–8004.
- Pallas, N.R., Pethica, B.A., 1985. Liquid-expanded to liquid-condensed transitions in lipid monolayers at the air/water interface. *Langmuir* 1, 509–513.
- Phillips, M.C., Chapman, D., 1968. Monolayer characteristics of saturated 1,2 diacyl phosphatidyl cholines (Lecithins) and phosphatidyl ethanolamines at the air/water interface. *Biochim. Biophys. Acta* 163, 301–313.
- Pusterla, J.M., Malfatti-Gasperini, A.A., Puentes-Martinez, X.E., Cavalcanti, L.P., Oliveira, R.G., 2017. Refractive index and thickness determination in Langmuir monolayers of myelin lipids. *Biochim. Biophys. Acta (BBA) - Biomembranes* 1859, 924–930.
- Ries Jr, H.E., 1979. Stable ridges in a collapsing monolayer. *Nature* 281, 287–289.
- Rothman, J.E., Lenard, J., 1977. Membrane asymmetry. *Science* 195, 743–753.
- Sabatini, K., Mattila, J.-P., Kinnunen, P.K.J., 2008. Interfacial behavior of cholesterol, ergosterol, and lanosterol in mixtures with DPPC and DMPC. *Biophys. J.* 95, 2340–2355.
- Salen, G., Shefer, S., 1983. Bile acids synthesis. *Ann. Rev. Physiol.* 45, 679–685.
- Schroeder, F., Nemezc, G., Wood, W.G., Joiner, C., Morrot, C., Ayraud-Jarrier, M., Devaux, P.F., 1991. Transmembrane distribution of sterol in the human erythrocyte. *Biochim. Biophys. Acta - Biomembranes* 1066, 183–192.
- Seoane, R., Miñones, J., Conde, O., Miñones Jr, J., 2000. Study of the interaction of cholesterol with potentially hypocholesterolemic substances in a monolayer form. *Colloids Surf. A Physicochem. Eng. Aspects* 174, 329–340.
- Steck, T.L., Ye, J., Lange, Y., 2002. Probing red cell membrane cholesterol movement with cyclodextrin. *Biophys. J.* 83, 2118–2125.
- Tabas, I., 2002. Cholesterol in health and disease. *J. Clin. Invest.* 110, 583–590.
- Takano, E., Ishida, Y., Iwahashi, M., Araki, T., Irimaya, K., 1997. Surface chemical and morphological study on monolayers of cholesterol, cholesterol, and their derivatives conjugated with amino acid. *Langmuir* 13, 5782–5786.
- Telesford, D.-M., Verreault, D., Reick-Mitrisiu, V., Alen, H.C., 2015. Reduced condensing and ordering effect by 7-ketocholesterol and 5b,6b-epoxycholesterol on Langmuir monolayers. *Langmuir* 31, 9859–9869.
- Viswanath, P., Suresh, K.A., 2004. Photoinduced phase separation and miscibility in the condensed phase of a mixed Langmuir monolayer. *Langmuir* 20, 8149–8154.
- Vollhardt, D., Fainerman, V.B., Siegel, S., 2000. Thermodynamics and textural characterization of DPPG phospholipid monolayers. *J. Phys. Chem. B* 104, 4115–4121.
- Wnętrzak, A., Chachaj-Brekiesz, A., Janiszewska-Sagan, M., Fidalgo Rodríguez, J.L., Miñones Conde, J., Dynarowicz-Latka, P., 2019. Crucial role of the hydroxyl group orientation in Langmuir monolayers organization – the case of 7-hydroxycholesterol epimers. *Colloids Surf. A* 563, 330–339.